Published OnlineFirst April 12, 2012; DOI:10.1158/1078-0432.CCR-11-1877

Clinical Cancer Research

Carbonic Anhydrase IX Promotes Tumor Growth and Necrosis *In Vivo* and Inhibition Enhances Anti-VEGF Therapy

Alan McIntyre, Shalini Patiar, Simon Wigfield, et al.

Clin Cancer Res 2012;18:3100-3111. Published OnlineFirst April 12, 2012.

Published OnlineFirst April 12, 2012; DOI:10.1158/1078-0432.CCR-11-1877

Cancer Therapy: Preclinical

Clinical Cancer Research

Carbonic Anhydrase IX Promotes Tumor Growth and Necrosis *In Vivo* and Inhibition Enhances Anti-VEGF Therapy

Alan McIntyre[1], Shalini Patiar[1], Simon Wigfield[1], Ji-liang Li[1], Ioanna Ledaki[1], Helen Turley[1,3], Russell Leek[1,3], Cameron Snell[1,3], Kevin Gatter[3], William S. Sly[4], Richard D. Vaughan-Jones[2], Pawel Swietach[2], and Adrian L. Harris[1]

Abstract

Purpose: Bevacizumab, an anti-VEGFA antibody, inhibits the developing vasculature of tumors, but resistance is common. Antiangiogenic therapy induces hypoxia and we observed increased expression of hypoxia-regulated genes, including carbonic anhydrase IX (CAIX), in response to bevacizumab treatment in xenografts. CAIX expression correlates with poor prognosis in most tumor types and with worse outcome in bevacizumab-treated patients with metastatic colorectal cancer, malignant astrocytoma, and recurrent malignant glioma.

Experimental Design: We knocked down CAIX expression by short hairpin RNA in a colon cancer (HT29) and a glioblastoma (U87) cell line which have high hypoxic induction of CAIX and overexpressed CAIX in HCT116 cells which has low CAIX. We investigated the effect on growth rate in three-dimensional (3D) culture and *in vivo*, and examined the effect of CAIX knockdown in combination with bevacizumab.

Results: CAIX expression was associated with increased growth rate in spheroids and *in vivo*. Surprisingly, CAIX expression was associated with increased necrosis and apoptosis *in vivo* and *in vitro*. We found that acidity inhibits CAIX activity over the pH range found in tumors (pK = 6.84), and this may be the mechanism whereby excess acid self-limits the build-up of extracellular acid. Expression of another hypoxia inducible CA isoform, CAXII, was upregulated in 3D but not two-dimensional culture in response to CAIX knockdown. CAIX knockdown enhanced the effect of bevacizumab treatment, reducing tumor growth rate *in vivo*.

Conclusion: This work provides evidence that inhibition of the hypoxic adaptation to antiangiogenic therapy enhances bevacizumab treatment and highlights the value of developing small molecules or antibodies which inhibit CAIX for combination therapy. *Clin Cancer Res; 18(11); 3100–11. ©2012 AACR.*

Introduction

The increased metabolic production, and impaired removal, of CO_2 and lactic acid can result in a highly acidic extracellular microenvironment (1, 2). Adaptation to this is crucial for cancer progression (3). Hypoxia-inducible factor (HIF), coordinates a shift in gene expression pattern, as part of the hypoxic response (4, 5). This includes increased expression of extracellular carbonic anhydrases IX (CAIX) and XII (CAXII; ref. 6). CAIX and CAXII expression has been identified in numerous cancer types and are generally associated with hypoxia (7–11). *CA9* expression is regulated by HIF-1α where the HRE/HIF-1α–binding site is located at −3 of −10 position in the promoter region of this gene (6, 12). CAIX and CAXII facilitate transmembrane removal of CO_2 (a weak acid) by hydrating extracellular CO_2 and thereby maintaining a steeper efflux gradient (13). We recently identified a major role for CAIX in regulating intracellular and extracellular pH in spheroids (14). CAIX expression maintained a more alkaline and uniform intracellular pH while producing a more acidic extracellular pH (14). We identified that the majority of cellular acid is excreted across the membrane in the form of CO_2 rather than lactic acid (15), highlighting the importance of extracellular CAs in maintaining favorable intracellular pH. The expression of CAIX is restricted in normal adult tissues (16, 17) and disruption of the mouse homolog of CAIX during development resulted in only gastric hyperplasia (18), therefore making it a good therapeutic target. CAIX is

Authors' Affiliations: [1]Molecular Oncology Laboratories, Department of Medical Oncology, Weatherall Institute of Molecular Medicine, [2]Department of Physiology, Anatomy and Genetics, Burdon Sanderson Cardiac Science Centre, [3]Nuffield Department of Clinical Laboratory Sciences, John Radcliffe Hospital, University of Oxford, Oxford, United Kingdom; and [4]St. Louis University School of Medicine, St. Louis, Missouri

Note: Supplementary data for this article are available at Clinical Cancer Research Online (http://clincancerres.aacrjournals.org/).

A. McIntyre and S. Patiar contributed equally to this work.

Corresponding Author: Adrian L. Harris, Weatherall Institute of Molecular Medicine, University of Oxford, Oxford OX3 9DS, United Kingdom. Phone: 44-01865-222457; Fax: 44-01865-222431; E-mail: aharris.lab@oncology.ox.ac.uk

doi: 10.1158/1078-0432.CCR-11-1877

Published OnlineFirst April 12, 2012; DOI:10.1158/1078-0432.CCR-11-1877

Translational Relevance

Although antiangiogenic therapy represents an important therapeutic strategy in cancer treatment, resistance is common. We identify increased expression of hypoxia-regulated CAIX in response to bevacizumab in xenografts. CAIX is a marker of poor prognosis in most tumor types and worse outcome in response to bevacizumab treatment. We showed that CAIX expression increased growth rate in xenografts, with increased expression of Ki-67 specifically in hypoxic areas of spheroids. CAIX was also associated with increased necrosis, a poor prognostic marker in many tumor types. We hypothesized that inhibiting this important hypoxia adaptation mechanism for regulating pH stress would sensitize cells to bevacizumab treatment. Indeed, CAIX knockdown or inhibition enhanced antiangiogenic therapy. This work shows the principle of targeting tumor hypoxic response mechanisms in combination with antiangiogenic therapy and highlights CAIX as a therapeutic target alone or in combination with anti-VEGF therapy.

a marker for poor clinical outcome in most cancer types (10, 19–21).

There is evidence of resistance to therapy in almost all anti-VEGF clinical trials (22, 23). Resistance mechanisms may include vascular regrowth due to additional proangiogenic factors such as Delta-like ligand 4 (DLL4; ref. 24); protection of the tumor vasculature by increasing recruitment of pericytes, which densely cover vessels or proangiogenic inflammatory cells, such as proangiogenic monocytic cells; or through co-opting normal vasculature by increased invasion into local tissues as reviewed by Bergers and Hanahan (25). In addition, antiangiogenic therapies induce hypoxia (26). This is likely to promote selection or adaptation of cells able to proliferate and survive in oxygen- and nutrient-deficient environments. Hypoxic adaptation occurs through HIF-1α stabilization and increased target gene expression. This hypoxic response could provide a further mechanism of resistance enabling tumors to overcome increased hypoxic conditions. CAIX expression was associated with poorer clinical outcome in response to antiangiogenic therapy (bevacizumab) in patients with metastatic colorectal cancer (27), malignant astrocytoma (28), and with worse progression-free survival in recurrent malignant glioma (29). VEGF, the target of bevacizumab and another target gene of HIF-1α, was not associated with worse outcome in these studies (27–29). These data suggest that CAIX may contribute to this angiogenesis-independent mechanism of resistance.

Two recent investigations of the role of CAIX in xenograft growth showed that CAIX knockdown by short hairpin RNA (shRNA) reduced xenograft tumor volume in one colon cancer cell line (30), one mouse breast cancer cell line, and one human breast cancer cell line (31). One of these studies showed upregulated CAXII expression in response to CAIX knockdown (26), where dual knockdown of both CAIX and CAXII reduced xenograft growth further (30). In this study, we constitutively knocked down CAIX expression in HT29 which have high levels of hypoxia-induced CAIX, to enable analysis of CAIX function. Conversely, we overexpressed *CA9* in HCT116 which have low levels of hypoxic CAIX and CAXII.

We found that the capacity of CAIX to hydrate CO_2 is negatively affected by acidity, thereby producing a self-limiting mechanism if excess acid accumulates. Overexpression of CAIX in HCT116 increased spheroid and xenograft growth rate. CAIX knockdown in HT29 cells reduced spheroid and xenograft growth rate. Surprisingly, CAIX expression increased necrosis in spheroids and xenografts (HT29 and HCT116) and increased markers for apoptosis in spheroids (HT29 and HCT116) and *in vivo* (HT29). CAIX expression also increased Ki-67 staining, a marker for proliferation (HT29). CAXII expression was upregulated in response to CAIX knockdown in spheroids and xenografts although not in 2-dimensional (2D) culture. We identified increased *CA9* expression in response to bevacizumab treatment in U87 (glioblastoma cell line) xenografts. Furthermore, we investigated the role of CAIX in resistance to bevacizumab treatment in HT29 and U87 xenografts. The results show an enhanced effect, significantly reducing growth rate.

Materials and Methods

Cell culture

Cells were maintained in a humidified incubator at 5% CO_2 and 37°C. For hypoxic exposure, cells were grown at 0.1% O_2, 5% CO_2, and 37°C. HCT116 were maintained in McCoy's 5A while HT29 and U87 were maintained in Dulbecco's Modified Eagle's Medium (DMEM) both supplemented with 10% FBS. For spheroid culture, aggregation was initiated by resuspending 4×10^6 cells in 250 mL of medium in 1 L spinner flasks (Techne MCS) spun at 40 rpm at 37°C, 5% CO_2 or as described previously (32).

Stable transfection

The following constructs were used to generate stable cell lines: human *CA9* cDNA (FLCA9; a gift from Dr. Jaromir Pastorek, Slovak Academy of Science, Bratislava, Slovak Republic) was cloned into pcDNA3.1(+) (Invitrogen). To knockdown *CA9* in HT29, the HuSH-29 shRNA targeting *CA9* (TR314250) and empty vector (R20003) were purchased from Origene. Cell lines were transfected with FuGENE 6 (Roche) according to manufacturer's instructions. To knockdown *CA9* in U87 a doxycycline inducible shCA9 (V3THS_363219) and shControl (shCTL; RHS4743) vectors were purchased from Thermo Scientific and lentivirus produced by the trans-lenti shRNA packaging kit (TLP4615) and cells transduced according to manufacturers instructions (Thermo Scientific). Cells were grown under selective pressure [HCT116, 0.4 mg/mL G418 (Invitrogen); HT29, 300 ng/mL puromycin; U87, 1 μg/mL puromycin (Invitrogen)] until no mock-transfected cells

Published OnlineFirst April 12, 2012; DOI:10.1158/1078-0432.CCR-11-1877

remained. Individual clones were isolated with cloning cylinders (Sigma).

Immunoblotting

Cell lysates were separated on 10% SDS-PAGE and transferred to polyvinylidene difluoride membrane. Primary antibodies were used at 1:1,000 unless otherwise stated. These were mouse anti-HIF-1α, (BD Transduction Laboratories), mouse anti-CA9 (Gift from J. Pastorek, Institute of Virology, Slovak Republic), goat anti-CA12 (R&D Systems), mouse anti-Na^+/K^+-ATPase (1:5,000; Abcam), and mouse anti-β-tubulin (Sigma). Appropriate secondary horseradish peroxidase (HRP)-linked antibodies were used (Dako). Immunoreactivity was detected with chemiluminescence (Amersham).

Quantitative PCR

RNA extraction and the quantitative PCR protocol have been described previously (33). Primer sequences: CA9 forward, CTTGGAAGAAATCGCTGAGG; CA9 reverse, TGGAAGTAGCGGCTGAAGTC; CA12 forward, GCTCTGAGCACACCGTCA; CA12 reverse, GGATAAAGGTCTGAGTTATAATGGACA; glyceraldehyde-3-phosphate dehydrogenase (GAPDH) forward, AGCCACATCGCTCAGACAC; GAPDH reverse, GCCCAATACGACCAAATCC.

Flow cytometry

Cells were detached and resuspended on ice in 100 μL of PBS, at a concentration of 2×10^6 cells per mL. Ten microliters of FITC Labeled CAIX (R&D systems) or isotype IgG antibody (R&D systems) was added and incubated for 1 hour at 4°C. Cells were washed with PBS and resuspended in 500 μL of PBS. Samples were analyzed by flow cytometry using a FACSCalibur flow cytometer (BD Biosciences) and CellQuest software (BD Biosciences).

CA activity assay

HCT116 cells were harvested to a total cell count of the order 10^7 to 10^8 in HEPES-buffered DMEM. Cells were lysed in 20 mmol/L HEPES, 20 mmol/L Mes, protease inhibitor (Roche), 30 mmol/L KCl, 0.5% Triton X, and a pH adjusted to the desired starting point between 6.5 and 8. The membrane fraction was separated from the cytosolic fraction by centrifugation at 100,000 rpm for 40 minutes. The pellet, containing the membrane fraction, was resuspended in fresh lysis buffer. The total CA activity was measured by a kinetic assay (as previously described; ref. 14). The pH sensitivity of CA activity was elucidated by adjusting lysis buffer pH to 6.5, 7.0, 7.5, and 8.0. CA activity was quantified relative to the spontaneous rate measured in lysis buffer only or in extracts treated with the broad spectrum CA inhibitor, acetazolamide (100 μmol/L). The CO_2 hydration rate constant was estimated by fitting experimental pH time courses with model predictions, run for different rate constants. The model consisted of 3 ordinary differential equations for pH, CO_2, and HCO_3^- and included pH sensitivity of the CO_2 hydration rate constant. Kinetic data were normalized to the protein content (per 1 mg/mL), measured by the Bradford assay (Biorad). The pH dependence of CA activity was fitted with a Hill equation, featuring the spontaneous hydration rate (k_{spont}), the maximum catalyzed activity (k_{max}), half-maximal pH (pK), and cooperativity (n or Hill number):

$$k_{hydration} = k_{spont} + k_{max} \times \frac{(10^{-pK})^n}{(10^{-pH})^n + (10^{-pK})^n}$$

Xenograft studies

Mice were housed at Cancer Research UK Laboratories (Clare Hall) and procedures were carried out under a Home Office license. Cells were trypsinized and washed twice in serum-free medium before inoculation in mice. Six- to 7-week-old female BALB/c *nu/nu* mice were injected subcutaneously in the lower flank with 100 μL Matrigel (BD Bioscience) and 1×10^7 cells suspended in 100 μL of serum-free medium. Tumor growth was monitored 3 times per week measuring the length (L), width (W), and height (H) of each tumor with calipers. Volumes were calculated from the formula $1/6 \times \pi \times L \times W \times H$. When tumors reached 1.44 cm^3 the mice were sacrificed by cervical dislocation. Ninety minutes before sacrifice, mice were injected intravenously with 2 mg of pimonidazole (hypoxyprobe-1; Chemicon International) as described previously (24). For bevacizumab treatment mice were injected intraperitoneally every 3 days (10 mg/kg), until sacrifice, once 2 of 5 mice from any group had xenografts which had reached 150 mm^3 in size. If required, doxycycline was given through the feed at 625 mg/kg *ad libitum* (SDS services) from the start of the experiment.

Immunohistochemistry

Immunohistochemistry was carried out as previously described (24). The following primary antibodies were used at room temperature for 1 hour; CAIX (M75, 1:50); HIF-1 (BD Biosciences; 1:100); pimonidazole (hypoxyprobe-1; Chemicon International; 1:50); CD34 (MCA1825; AbD Serotec; 1:50), cleaved caspase-3 (RnD systems; 1:2,000), CAXII (1:1,000; ref. 34), and Ki-67 (M7240; Dako; 1:50). Slides were incubated with the anti-rabbit/anti-mouse secondary antibody (Dako) for 30 minutes at room temperature and washed in PBS. 3,3′-Diaminobenzidine (DAB; Dako) was applied to the sections for 7 minutes. The slides were counterstained by immersing in hematoxylin solution (Sigma-Aldrich) for 20 seconds and mounted with Aquamount (VWR). Secondary-only control staining was done routinely, these were negative. One section from each xenograft was analyzed for each stain. Slides were scored by 2 researchers blinded to groupings (as a percentage or index based on intensity and percentage positive) or analyzed quantitatively by image analysis in imageJ using color deconvolution as described previously (35). Where scores differed, sections were reviewed and a consensus result was decided.

Statistics

Statistical analysis including the Student t test, one-way ANOVA, and linear regression of log transformed growth data were carried out as appropriate with GraphPad Prism 4.0b.

Published OnlineFirst April 12, 2012; DOI:10.1158/1078-0432.CCR-11-1877

Results

Validation of stable transfectants

HCT116 cells were transfected with the *CA9* coding sequence (FLCA9) or empty vector (EV). CAIX was overexpressed relative to empty vector shown by immunoblot and flow cytometry (Fig. 1A).

HT29 was transfected with an shRNA targeting *CA9* (shCA9) or empty vector. CAIX knockdown in shCA9 was shown by quantitative PCR and immunoblot compared with empty vector (Fig. 1B). The expression of *CA9* in shCA9 was 6% the empty vector levels at 0.1% O_2 for 72 hours (***, $P < 0.001$, $n = 3$).

U87 cells were transduced with an shCA9 or a nontargeting shRNA (shCTL). *CA9* knockdown in shCA9 was shown by quantitative PCR (***, $P < 0.001$, $n = 3$; Fig. 1C) and by immunoblotting at a range of doxycycline concentrations (Fig. 1D).

Acidity inhibits CAIX activity *in vitro* in HCT116

HCT116 FLCA9 and empty vector membrane extracts were prepared and tested for CA activity. The subcellular fractionation was assessed by immunoblotting the membrane fraction for Na^+/K^+-ATPase, a membrane-specific protein (Fig. 1E). Membrane extracts from empty

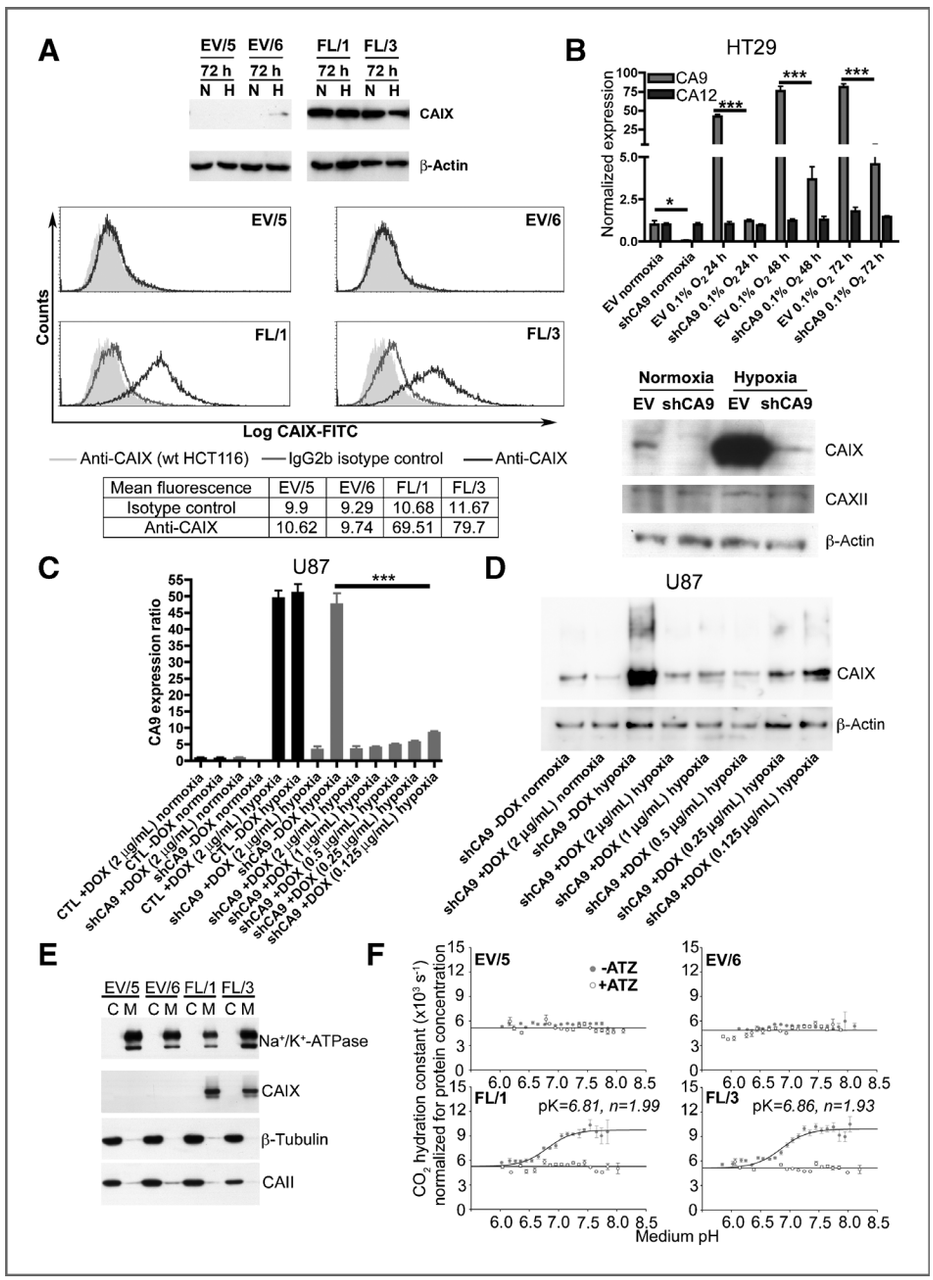

Figure 1. Analysis of CAIX expression and activity. A, CAIX expression in HCT116 clones by immunoblot (top) and fluorescence-activated cell-sorting (FACS) analysis (bottom). B, *CA9* and *CA12* expression in HT29 in normoxic and 0.1% O_2 (top). ***, $P < 0.001$; *, $P < 0.05$, $n = 3$, hypoxia. CAIX and CAXII expression in normoxic and 0.1% O_2, 72 hours (bottom). C, *CA9* expression in U87 shCTL and shCA9 pools in normoxia and 0.1% O_2 (hypoxia; 72 hours) measured by (C) quantitative PCR and (D) immunoblot. E, immunoblot of cytoplasmic (C) and membrane (M) fraction of HCT116 clones. F, CO_2 hydration rate constant of HCT116 clones at a range of pH ± acetazolamide (ATZ). Immunoblots are representative of 3 blots. Error bars represent SD. FITC, fluorescein isothiocyanate.

Published OnlineFirst April 12, 2012; DOI:10.1158/1078-0432.CCR-11-1877

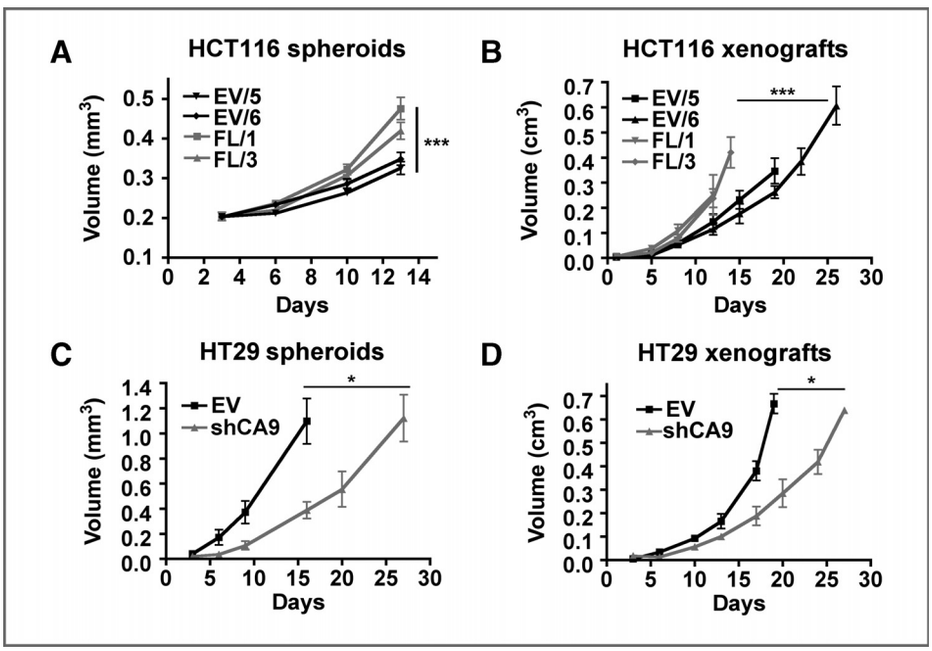

Figure 2. CAIX increases growth rate in spheroids and xenografts. A, spheroid growth curves of HCT116 (***, $P < 0.001$, $n = 3$). B, xenograft growth curves of HCT116 (***, $P < 0.001$, $n = 5$). C, spheroid growth curves of HT29 (*, $P < 0.05$, $n = 3$). D, xenograft growth curves of HT29 (*, $P < 0.05$, $n = 5$). Error bars represent SD.

vector cells showed hydration at the spontaneous rate, with similar CO_2 hydration rates in the presence of acetazolamide, a CA inhibitor. In FLCA9, CAIX was catalytically active in the membrane fraction and inhibition to basal empty vector levels occurred in the presence of acetazolamide. CA activity was markedly reduced by decreasing pH, with CA activity almost completely inhibited at pH 6.0 and a pK (pH for half-maximum rate) between 6.81 and 6.86 (Fig. 1F). Best-fitting Hill curves to the pH-sensitivity data yielded Hill cooperativity numbers near 2 for full-length CAIX. As a consequence of this, the pH sensitivity of CAIX to pH is steeper than for other CA isoforms (36).

CAIX expression increases growth rate in 3D culture and *in vivo*

We found a significant increase in growth rate in HCT116 FLCA9 spheroids (***, $P < 0.001$, $n = 3$; Fig. 2A) and xenografts (***, $P < 0.001$, $n = 10$; Fig. 2B) compared with empty vector.

CAIX knockdown reduced the growth rate of HT29 spheroids (*, $P < 0.05$, $n = 3$; Fig. 2C) and xenografts (*, $P < 0.05$, $n = 5$; Fig. 2D) compared with empty vector.

CAIX expression promotes necrosis, apoptosis, and proliferation in spheroid culture and *in vivo*

We characterized the spheroids and xenograft tumors for several immunohistologic markers related to cell survival and angiogenesis.

CAIX expression

In HCT116 spheroids, the percentage of CAIX-positive cells was greater in FLCA9 (95%) than empty vector (5%; ***, $P < 0.001$, $n = 5$; Fig. 3A). Similarly in HCT116 xenografts, the percentage of CAIX-positive cells was greater in FLCA9 (FL/1, 55% and FL/3, 75.5%) than empty vector (EV; EV/5, 12.5% and EV/6, 13.5%; ***, $P < 0.001$, $n = 10$; Fig. 4A).

In HT29 spheroids, CAIX expression was decreased in shCA9 (2.5%) compared with empty vector (18%; ***, $P < 0.001$, $n = 5$; Fig. 3B). The same was true in the xenografts shCA9 (6%) compared with empty vector (17%; ***, $P < 0.001$, $n = 5$; Fig. 4B).

Necrosis

In HCT116 spheroids, the proportion of necrosis was higher in FLCA9 (15%) than in empty vector (5%; *, $P < 0.01$, n = 5; Fig. 3A). The proportion of necrosis was significantly higher in FLCA9 HCT116 xenografts (FL/1, 39.5% and FL/3, 28.6%) than in empty vector (EV/5, 6.9% and EV/6, 12.1%; *, $P < 0.05$, $n = 10$; Fig. 4A).

Conversely in the HT29 spheroids and xenografts, the shCA9 had less necrosis (spheroids, 19% and xenografts, 13%) than empty vector [spheroids, 36% and xenografts, 35%; spheroids, ***, $P < 0.001$, $n = 5$ (Fig. 3B) and xenografts, *, $P < 0.05$, $n = 5$ (Fig. 4B)].

Apoptosis

HCT116 FLCA9 spheroids showed increased apoptosis compared with empty vector as determined by immunostaining for activated caspase-3 (2.9% and 6.0%, respectively, ***, $P < 0.001$, $n = 5$; Fig. 3A) although this was not found in the xenografts (Fig. 4A).

Increased apoptosis was found in the HT29 empty vector spheroids and xenografts compared with shCA9 (spheroids, 9% and 5%; ***, $P < 0.001$, $n = 5$; Fig. 3B and xenografts; *, $P < 0.05$, $n = 5$; Fig. 4B).

Published OnlineFirst April 12, 2012; DOI:10.1158/1078-0432.CCR-11-1877

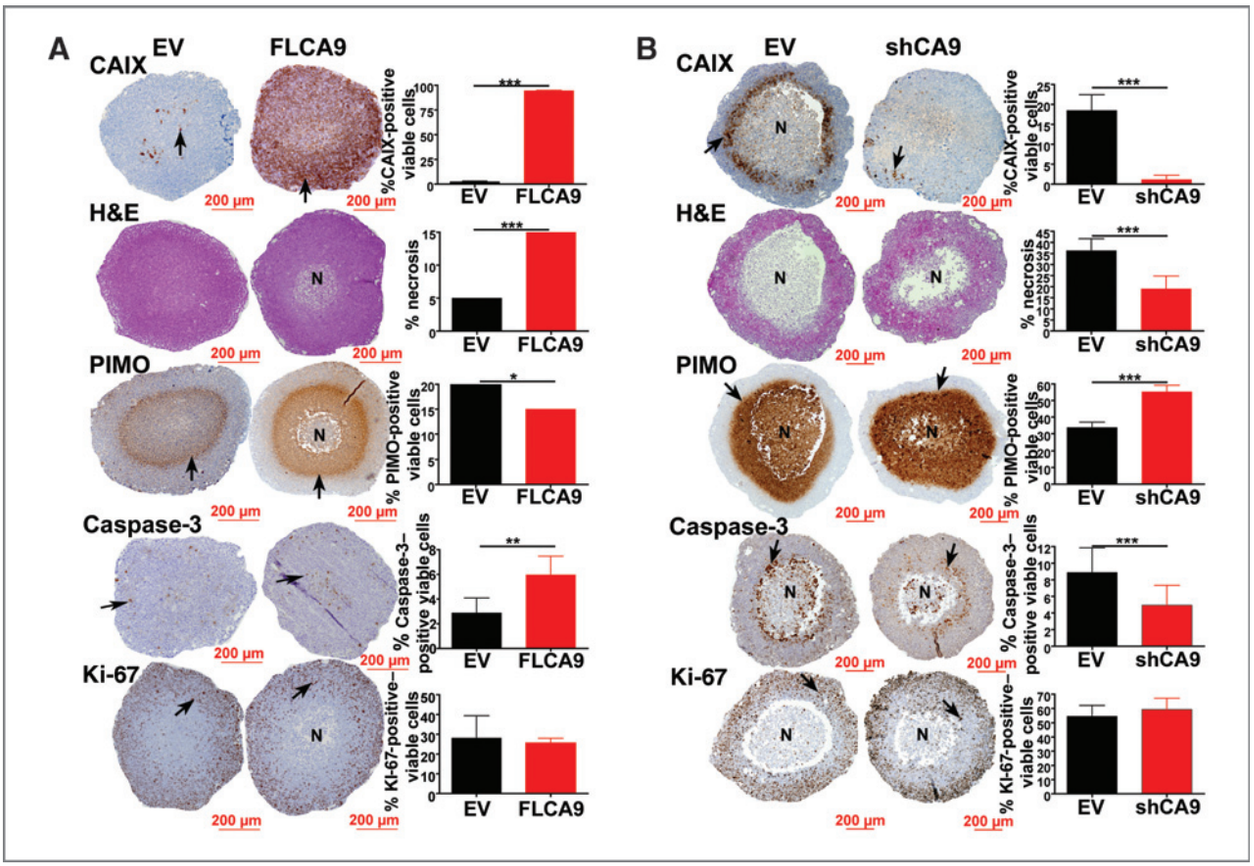

Figure 3. CAIX expression is associated with increased necrosis and apoptosis in spheroid culture. A, representative immunohistochemical images and bar chart of scoring in HCT116 FLCA9 and empty vector (EV) spheroids. CAIX expression, percentage of necrosis, percentage of pimonidazole (PIMO), and caspase-3 staining were significantly different between empty vector and FLCA9 spheroids. B, representative immunohistochemical images and bar charts of scoring of HT29 empty vector and shCA9 spheroids. CAIX expression, percentage of necrosis, percentage of pimonidazole, and cleaved caspase-3 staining were significantly different between empty vector and shCA9. CAIX, pimonidazole, caspase-3, and Ki-67 expression staining are shown in dark brown. Hematoxylin and eosin (H&E), dark pink denotes viable tissue, light pink denotes necrosis. Error bars represent SD. N denotes areas of necrosis. Arrows point to positive staining (***, $P < 0.001$; **, $P < 0.01$; *, $P < 0.05$, $n = 5$).

Ki-67

In HT29 xenografts, the percentage of Ki-67–positive nuclei was higher in empty vector (89%) than in shCA9 (55%, ***, $P < 0.001$, $n = 5$; Fig. 4B). In HT29 spheroids, Ki-67 positivity was higher in hypoxic areas in empty vector (32%) than in shCA9 (15%, ***, $P < 0.001$, $n = 5$; Fig. 5A). Hypoxic areas were defined by pimonidazole staining. There was no difference in Ki-67 positivity in HCT116, FLCA9 or empty vector spheroids (Fig. 3A), or xenografts (Fig. 4A).

Pimonidazole

Reduced pimonidazole staining was associated with CAIX expression in spheroids, HCT116 FLCA9 (15%) and empty vector (20%, *, $P < 0.05$, $n = 5$; Fig. 3A), HT29 empty vector (32%), and shCA9 (55%, ***, $P < 0.001$, $n = 5$; Fig. 3B). This was due to the increase in necrosis in hypoxic areas of CAIX-positive spheroids, which reduced the amount of viable hypoxic tissue. CAIX expression did not effect the distance from the edge of the spheroids that pimonidazole staining began. There was no difference in pimonidazole staining in xenografts in HCT116 (Fig. 4A) or in HIF-1α staining in HT29 (Fig. 4B).

CD34

CAIX expression did not affect CD34 staining, a marker for blood vessels in xenografts in HCT116 (Fig. 4A) and HT29 (Fig. 4B).

CAIX expression results in more viable tumor cells

CAIX increased growth rate while also increasing necrosis. Therefore, it was unclear whether CAIX expression increased the amount of viable tumor tissue at a given time point. To calculate the volume of the viable tumor, we subtracted the percentage of necrotic tumor (determined by histology, Figs. 3 and 4) from the endpoint volumes of the xenografts and spheroids expressing CAIX. These viable tumor volumes of the CAIX expressors were greater than the volumes of the spheroids and xenografts which lacked CAIX expression at the same

Published OnlineFirst April 12, 2012; DOI:10.1158/1078-0432.CCR-11-1877

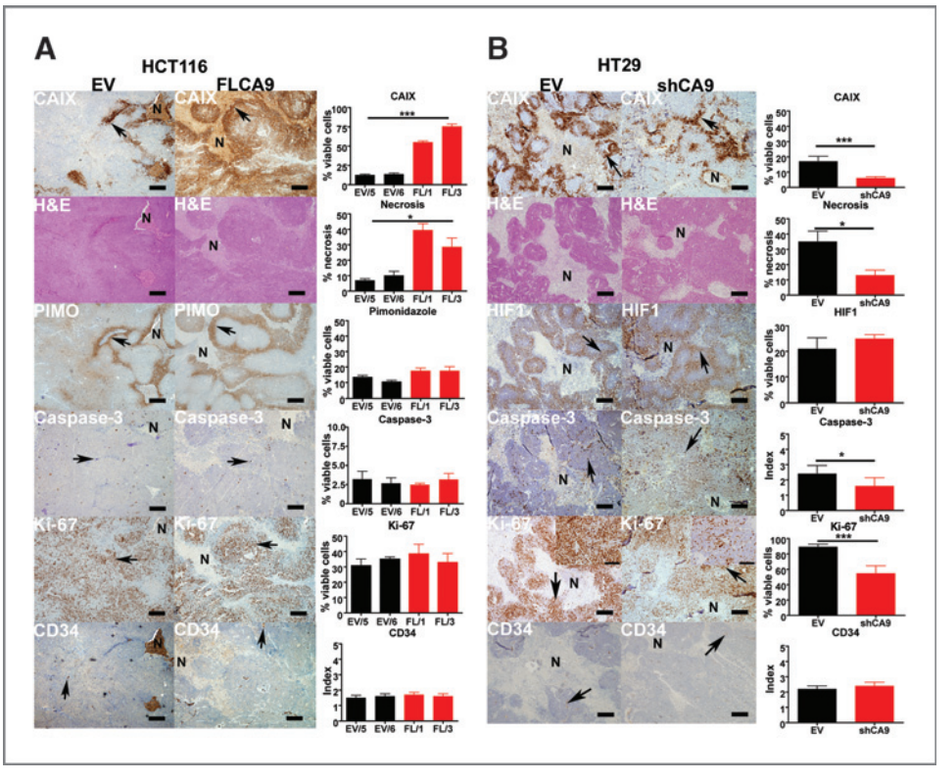

Figure 4. CAIX expression is associated with increased necrosis in HCT116 xenografts and increased necrosis, apoptosis, and proliferation in HT29 xenografts. A, representative immunohistochemical images of HCT116 empty vector (EV) and FLCA9 xenografts and bar chart of scoring. CAIX expression and proportion of necrosis were significantly different between empty vector and FLCA9. B, representative immunohistochemical images of HT29 empty vector and shCA9 xenografts and bar chart of scoring. CAIX expression, proportion of necrosis, cleaved caspase-3, and Ki-67 expression were significantly different between empty vector and shCA9. CAIX, HIF-1, cleaved caspase-3, Ki-67, and CD34 expression staining is shown in dark brown. H&E, dark pink denotes viable tissue, the light pink stain denotes necrosis. Error bars represent SD. N denotes areas of necrosis. Arrows point to positive staining. Scale bars represent 200 μm. Ki-67 images have a top right × 20 inset image with scale bars representing 100 μm. (***, $P < 0.001$; *, $P < 0.05$, $n = 5$).

time point. However, the latter were allowed to continue to grow to assess final growth curves.

This analysis revealed that the CAIX expressors had increased viable tumor volume in HCT116 xenografts (66% more viable tumor at day 14, ***, $P < 0.01$, $n = 10$) and spheroids (19% more viable tumor at day 13, **, $P < 0.01$, $n = 5$) and HT29 xenografts (52% more tumor tissue at day 20, $P < 0.05$, $n = 5$) and spheroids (81% more viable tumor at day 16, *, $P < 0.01$, $n = 5$; Supplementary Fig. S1).

Although we acknowledge a likely overestimation in the amount of viable tumor in the CAIX-deficient groups (HCT116 empty vector and HT29 shCA9), as necrosis was not subtracted from these volumes, this would only make the results more significant. Necrosis was not subtracted from the CAIX-deficient groups (HCT116 empty vector and HT29 shCA9) because data on the amount of necrosis was only available at the time of sacrifice of these controls, not the earlier date on which the CAIX expressors were ended.

CAIX knockdown increases CAXII expression in 3D culture and *in vivo* but not in 2D culture in HT29

In HT29, no effect was identified on CAXII RNA or protein levels in response to CAIX knockdown in 2D culture (Fig. 1B). In 3-dimensional (3D) culture CAIX knockdown increased *CA12* expression at the RNA (by ~2-fold, $P < 0.05$, $n = 5$; Fig. 5B) and protein level by immunohistochemistry (from 1% to 2% of cells; ***, $P < 0.001$, $n = 5$; Fig. 5D). *In vivo* CAIX knockdown did not increase *CA12* RNA expression (Fig. 5C) but did increase CAXII protein expression in shCA9 (5%) compared with empty vector (2%; *, $P < 0.05$, $n = 5$; Fig. 5E).

Knockdown of CAIX enhances antiangiogenic therapy reducing growth rate *in vivo*

We identified that *CA9* expression was increased (***, $P < 0.001$, $n = 5$) in response to bevacizumab treatment with material from a previous xenograft experiment using, the glioblastoma cell line, U87 (ref. 24; Supplementary Fig. S2). HT29 empty vector and shCA9 were grown as xenografts with and without bevacizumab treatment (Fig. 6A). The shCA9 clone grew more slowly than the empty vector clone as before (75.9% the growth rate of the empty vector; *, $P < 0.05$, $n = 5$). Bevacizumab treatment also reduced xenograft growth rate (68% the rate of empty vector control; *, $P < 0.05$, $n = 5$). The HT29 shCA9 clones treated with bevacizumab grew significantly more slowly

Published OnlineFirst April 12, 2012; DOI:10.1158/1078-0432.CCR-11-1877

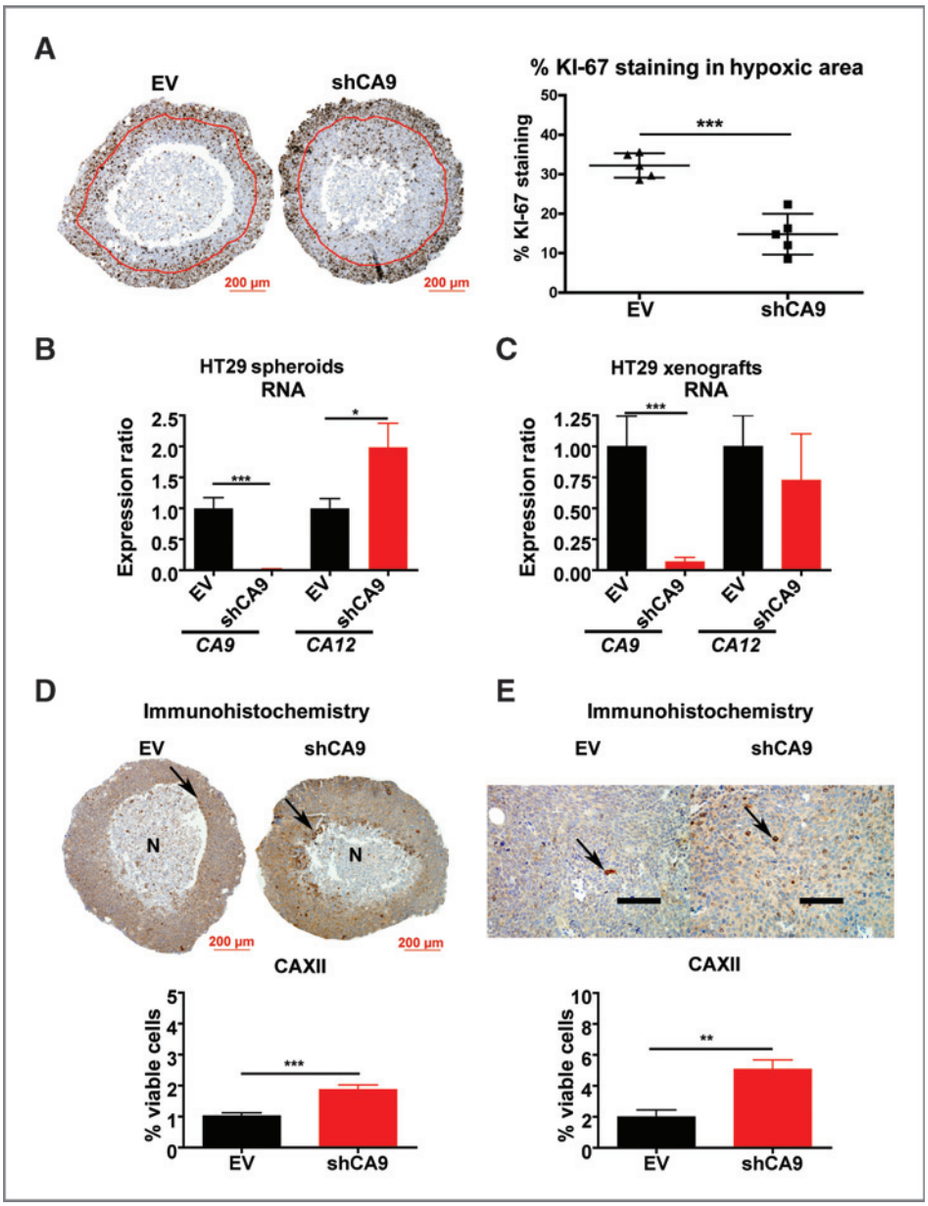

Figure 5. CAIX knockdown in HT29 reduces Ki-67 positivity in the hypoxic fraction of spheroids and increases CAXII expression in 3D culture and *in vivo*. A, examples of HT29 empty vector (EV) and shCA9 spheroids stained for Ki-67. Red lines denote the area of central hypoxia. A graph of the percentage of Ki-67 positivity inside the hypoxic core of the HT29 empty vector and shCA9 spheroids. B, analysis of *CA9* and *CA12* RNA expression in HT29 empty vector and shCA9 spheroids. C, analysis of *CA9* and *CA12* RNA expression in HT29 empty vector and shCA9 xenografts. D, analysis of CAXII expression by immunohistochemistry with representative images of empty vector and shCA9 spheroids (top) and a bar chart of the scoring (bottom). E, analysis of CAXII expression by immunohistochemistry with representative images of empty vector and shCA9 xenografts (top) and a bar chart of the scoring (bottom). CAXII expression staining is shown in dark brown. N denotes areas of necrosis. Arrows point to positive staining. Scale bars represent 100 μm. (***, $P < 0.001$; *, $P < 0.05$, $n = 5$).

than shCA9-untreated xenografts or empty vector bevacizumab-treated xenografts (37% the growth rate of untreated empty vector; *, $P < 0.05$, $n = 5$; Fig. 6A). This was at least an additive reduction in growth rate. shCA9 xenografts had reduced CAIX expression compared with empty vector clones when treated with vehicle (PBS; *, $P < 0.01$, $n = 5$) and with bevacizumab (***, $P < 0.001$, $n = 5$; Supplementary Fig. S3). HT29 cells were also treated with acetazolamide in combination with bevacizumab. Acetazolamide or bevacizumab treatment alone did not significantly reduce growth rate however, both in combination, reduced growth significantly compared with untreated (*, $P < 0.05$, $n = 5$) or bevacizumab-treated alone (*, $P < 0.05$, $n = 3$; Fig. 6B).

U87 xenografts with doxycycline-inducible shCA9 were treated with bevacizumab. The shCA9 without doxycycline and the shCTL with or without doxycycline xenografts grew at the same rate (Fig. 6C). *CA9* knockdown (33% reduction, $P < 0.05$, $n = 5$) or bevacizumab treatment alone (38% reduction, $P < 0.05$, $n = 5$) significantly reduced xenografts growth rate. *CA9* knockdown and bevacizumab treatment in combination significantly reduced growth rate further (>50%), more than *CA9* knockdown (*, $P < 0.05$, $n = 5$) or bevacizumab treatment (*, $P < 0.05$, $n = 5$) alone.

Bevacizumab treatment reduced the number of blood vessels in the HT29 xenografts as determined by CD34 staining [empty vector: $P < 0.05$, $n = 5$; shCA9: $P < 0.05$,

Published OnlineFirst April 12, 2012; DOI:10.1158/1078-0432.CCR-11-1877

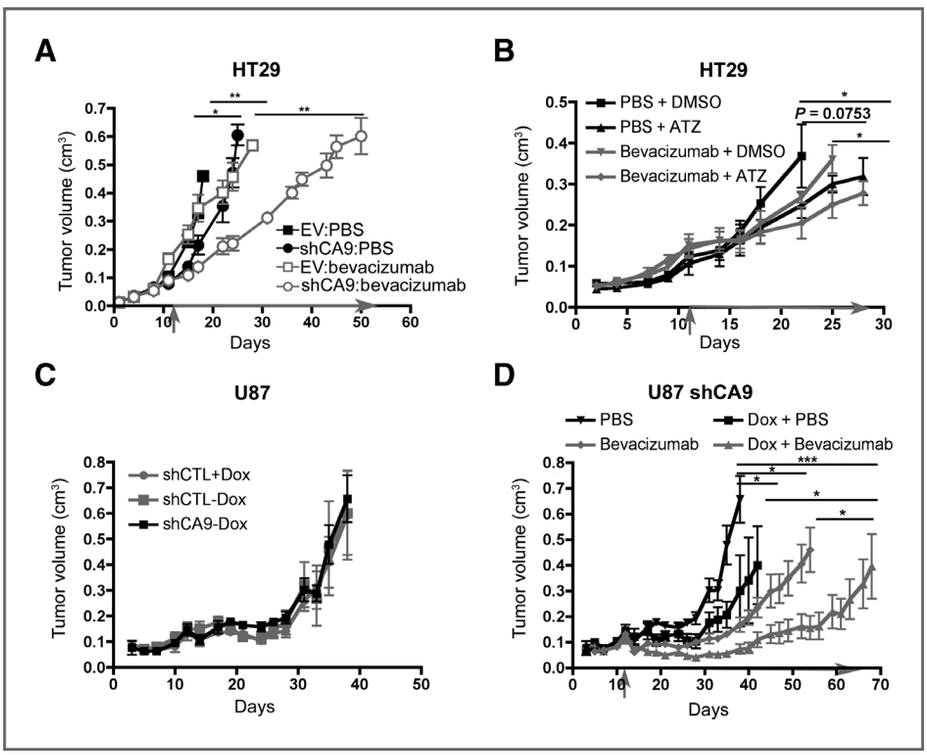

Figure 6. CAIX knockdown enhances bevacizumab treatment in xenografts. A, xenograft growth curves of HT29 clones ± bevacizumab treatment. B, xenograft growth curves of HT29 wt ± acetazolamide (ATZ) ± bevacizumab treatment. C, xenograft growth curves of U87 doxycycline (Dox)-inducible shCTL ± Dox and shCA9 − Dox xenografts. D, xenograft growth curves of U87 doxycycline (Dox)-inducible shCA9 ± Dox ± bevacizumab. Arrows denote the start of bevacizumab treatment and/or acetazolamide treatment at 150 mm^3 xenograft volume. (***, $P < 0.001$; **, $P < 0.01$; *, $P < 0.05$, $n = 5$).

$n = 5$; vehicle: *, $P < 0.05$, $n = 5$; acetazolamide (ATZ): *, $P < 0.01$, $n = 5$; Supplementary Figs. S3 and S4]. Bevacizumab treatment increased the amount of hypoxia in xenografts as determined by HIF-1α immunostaining (empty vector: *, $P < 0.05$, $n = 5$; shCA9: *, $P < 0.01$, $n = 5$). CAIX immunostaining (empty vector: ***, $P < 0.001$, $n = 5$; vehicle: *, $P < 0.05$, $n = 5$; ATZ: **, $P < 0.01$, $n = 5$), the amount of necrosis (shCA9: *, $P < 0.01$, $n = 5$) and apoptosis as determined by caspase-3 activation (empty vector: ***, $P < 0.01$, $n = 5$; shCA9: *, $P < 0.05$, $n = 5$′ Supplementary Figs. S3 and S4) was also increased with bevacizumab treatment.

Discussion

We recently highlighted the importance of CAIX in regulating intracellular and extracellular pH in spheroids (14, 15, 37, 38). In addition, the proteoglycan domain of CAIX has previously been linked to negative regulation of cell adhesion through modulation of β-catenin and E-cadherin interactions (39), whereas the intracellular domain has been shown to contribute to AKT activation (40). To understand the role of CAIX in spheroids and *in vivo*, we knocked down CAIX in HT29 cells, which have high levels of CAIX under hypoxic stress. Several cell lines and human tumors have low levels of CAIX expression or induction by hypoxia, and the HCT116 cells provided an opportunity to investigate the role of CAIX when uniformly expressed in a tumor. Further to this, we examined the role of CAIX in resistance to severe hypoxia induced by bevacizumab treatment in HT29 and U87 cells.

We found that CAIX catalytic activity is inhibited by low pH and was half-maximal (i.e., the pK) at pH approximately 6.8. This is lower than the typical value for other CA isoforms (36), but in the range of extracellular pH measured in human tumors (pH6.5–6.8; refs. 41, 42). Consequently, H^+ ions, produced by CO_2 hydration in the tumor milieu, can exert an important autoinhibitory effect on CAIX. The pH dependence of CAIX activity showed a cooperativity of approximately 2 [higher than reported for a truncated recombinant CAIX (ref. 43) and for other CA isoforms (ref. 36)], making CAIX activity more H^+ sensitive as pH approaches the enzyme's pK. CAIX's relatively low pK will allow the tumor to attain a more acidic extracellular pH, whereas higher cooperativity may protect from excessive acidification by strengthening the autoinhibitory H^+ effect below a critical pH. Although there is pH inhibition of CAIX activity, it is not autoinhibited abruptly, but gradually, and therefore significant activity is still measurable at pH 6.5. We have modeled the relationship between CA activity and extracellular pH (15).We showed that "basal" CAIX activity would have to be very mild to be completely switched off by extracellular H^+ ions.

We show that CAIX knockdown reduced the growth rate of xenografts as has been reported in 2 recent studies (26, 31). In addition, we identify the converse, whereby overexpression of CAIX in HCT116 increased growth rate. However, we identified, for the first time, that CAIX expression was associated with increased necrosis. This was

Published OnlineFirst April 12, 2012; DOI:10.1158/1078-0432.CCR-11-1877

surprising as we initially expected CAIX to reduce necrosis by improving intracellular pH control. The overall effect of this was increased tumor volume with more viable tumor and more necrosis at the same time point in the CAIX expressors, of both HCT116 and HT29 cell lines. The increase in apoptosis associated with CAIX offers a mechanism to explain the increased pathologic necrosis.

We hypothesize that the necrosis may represent regions where CAIX expression has maintained a high level of proliferation (as shown in Fig. 5A) through the maintenance of a more uniformly alkaline intracellular pH. This would increase metabolic demand and deplete substrates in the hypoxic milieu. We previously identified that necrosis also induces infiltration of macrophages which may contribute to an aggressive tumor phenotype (44, 45) and necrosis is associated with poor prognosis in many cancer types including colorectal cancer (46). So the well-recognized observation of CAIX staining around necrotic areas may reflect a causative role in necrosis.

CAIX expression was associated with Ki-67 positivity in HT29, particularly in the hypoxic areas in HT29 spheroids. This is in agreement with data that CAIX maintains an intracellular environment conducive for growth under hypoxic conditions. CAIX expression increased growth in HCT116 spheroids and xenografts, however there was no difference in Ki-67 staining. While Ki-67 stains positive proliferative cells, staining does not relate to the time required for an intermitotic cycle completion (47).

A recent study identified CAXII upregulation in response to CAIX knockdown in 2D culture at the RNA and protein level (30). We have identified CAXII upregulation in response to CAIX knockdown in spheroids and *in vivo*, but not in 2D culture. The cause of this difference requires further study, but it may be related to differences in pH or oxygen tension between 2D and 3D culture.

We investigated CAIX knockdown in combination with antiangiogenic therapy (bevacizumab) in 2 tumor types. CAIX was recently associated with poor outcome in patients with metastatic colorectal treated with bevacizumab (27). Here, we show that CAIX knockdown and bevacizumab treatment acted additively in reducing xenograft growth rate in the colon adenocarcinoma cell line HT29 and synergistically in the glioblastoma cell line U87. In addition, the CA inhibitor acetazolamide enhanced bevacizumab treatment in HT29 xenografts. Our results provide experimental evidence that is consistent with previous immunohistologic data (27–29), showing that CAIX is part of a resistance mechanism that enables tumors to adapt to the increased hypoxia induced by bevacizumab treatment. On the basis of these data, detection of CAIX induction levels, possibly detected in blood serum or urine (48), in response to bevacizumab could help in predicting outcome to bevacizumab treatment. This highlights also the general principle of targeting the hypoxia survival mechanisms in combination with bevacizumab treatment, particularly given the chemotherapy and radiotherapy resistance of such hypoxic areas.

The effect of CAIX knockdown, reducing xenograft tumor growth alone, and at least additively in combination with antiangiogenic therapy, and the association between CAIX expression and increased necrosis, identifying a further mechanism to explain CAIX association with poorer outcome, highlight potential mechanisms by which CAIX inhibitory therapeutics, such as antibodies (49) and small-molecular inhibitors (50), may be used optimally.

Disclosure of Potential Conflicts of Interest

No potential conflicts of interest were disclosed.

Authors' Contributions

Conception and design: A. McIntyre, S. Wigfield, J.-L. Li, A.L. Harris
Development of methodology: A. McIntyre, S. Patiar, S. Wigfield, J.-L. Li, H. Turley, C. Snell, K.C. Gatter, R.D. Vaughan-Jones, A.L. Harris
Acquisition of data (provided animals, acquired and managed patients, provided facilities, etc.): A. McIntyre, S. Patiar, S. Wigfield, J.-L. Li, I. Ledaki, R. Leek, K.C. Gatter, R.D. Vaughan-Jones, P. Swietach
Analysis and interpretation of data (e.g., statistical analysis, biostatistics, computational analysis): A. McIntyre, S. Wigfield, J.-L. Li, I. Ledaki, R. Leek, C. Snell, K.C. Gatter, P. Swietach, A.L. Harris
Writing, review, and/or revision of the manuscript: A. McIntyre, S. Patiar, S. Wigfield, J.-L. Li, R. Leek, K.C. Gatter, W.S. Sly, P. Swietach, A.L. Harris
Administrative, technical, or material support (i.e., reporting or organizing data, constructing databases): A. McIntyre, S. Patiar, S. Wigfield, H. Turley, R. Leek, K.C. Gatter
Study supervision: A. McIntyre, K.C. Gatter, A.L. Harris
Provided reagent: W.S. Sly

Grant Support

This work was supported by funds from Cancer Research UK, EU Framework 7 Metoxia (to A.L. Harris), The Royal Society, Medical Research Council (to P. Swietach), and NIH grant GM034182 (to W.S. Sly).

The costs of publication of this article were defrayed in part by the payment of page charges. This article must therefore be hereby marked *advertisement* in accordance with 18 U.S.C. Section 1734 solely to indicate this fact.

Received July 20, 2011; revised March 20, 2012; accepted March 29, 2012; published OnlineFirst April 12, 2012.

References

1. Raghunand N, Gatenby RA, Gillies RJ. Microenvironmental and cellular consequences of altered blood flow in tumours. Br J Radiol 2003;76 Spec No 1:S11–22.
2. Gatenby RA, Gillies RJ. Why do cancers have high aerobic glycolysis? Nat Rev Cancer 2004;4:891–9.
3. Pouyssegur J, Dayan F, Mazure NM. Hypoxia signalling in cancer and approaches to enforce tumour regression. Nature 2006;441:437–43.
4. Semenza GL. Regulation of mammalian O2 homeostasis by hypoxia-inducible factor 1. Annu Rev Cell Dev Biol 1999;15:551–78.
5. Wykoff CC, Pugh CW, Harris AL, Maxwell PH, Ratcliffe PJ. The HIF pathway: implications for patterns of gene expression in cancer. Novartis Found Symp 2001;240:212–25; discussion 225–31.
6. Wykoff CC, Beasley NJ, Watson PH, Turner KJ, Pastorek J, Sibtain A, et al. Hypoxia-inducible expression of tumor-associated carbonic anhydrases. Cancer Res 2000;60:7075–83.
7. Beasley NJ, Wykoff CC, Watson PH, Leek R, Turley H, Gatter K, et al. Carbonic anhydrase IX, an endogenous hypoxia marker, expression in head and neck squamous cell carcinoma and its relationship to

Published OnlineFirst April 12, 2012; DOI:10.1158/1078-0432.CCR-11-1877

hypoxia, necrosis, and microvessel density. Cancer Res 2001;61: 5262–7.
8. Olive PL, Aquino-Parsons C, MacPhail SH, Liao SY, Raleigh JA, Lerman MI, et al. Carbonic anhydrase 9 as an endogenous marker for hypoxic cells in cervical cancer. Cancer Res 2001;61: 8924–9.
9. Loncaster JA, Harris AL, Davidson SE, Logue JP, Hunter RD, Wycoff CC, et al. Carbonic anhydrase (CA IX) expression, a potential new intrinsic marker of hypoxia: correlations with tumor oxygen measurements and prognosis in locally advanced carcinoma of the cervix. Cancer Res 2001;61:6394–9.
10. Hui EP, Chan AT, Pezzella F, Turley H, To KF, Poon TC, et al. Coexpression of hypoxia-inducible factors 1alpha and 2alpha, carbonic anhydrase IX, and vascular endothelial growth factor in nasopharyngeal carcinoma and relationship to survival. Clin Cancer Res 2002;8:2595–604.
11. Swinson DE, Jones JL, Richardson D, Wykoff C, Turley H, Pastorek J, et al. Carbonic anhydrase IX expression, a novel surrogate marker of tumor hypoxia, is associated with a poor prognosis in non-small-cell lung cancer. J Clin Oncol 2003;21:473–82.
12. Kaluz S, Kaluzova M, Liao SY, Lerman M, Stanbridge EJ. Transcriptional control of the tumor- and hypoxia-marker carbonic anhydrase 9: a one transcription factor (HIF-1) show? Biochim Biophys Acta 2009;1795:162–72.
13. Swietach P, Wigfield S, Supuran CT, Harris AL, Vaughan-Jones RD. Cancer-associated, hypoxia-inducible carbonic anhydrase IX facilitates CO2 diffusion. BJU Int 2008;101 Suppl 4:22–4.
14. Swietach P, Wigfield S, Cobden P, Supuran CT, Harris AL, Vaughan-Jones RD. Tumor-associated carbonic anhydrase 9 spatially coordinates intracellular pH in three-dimensional multicellular growths. J Biol Chem 2008;283:20473–83.
15. Swietach P, Patiar S, Supuran CT, Harris AL, Vaughan-Jones RD. The role of carbonic anhydrase 9 in regulating extracellular and intracellular ph in three-dimensional tumor cell growths. J Biol Chem 2009; 284:20299–310.
16. Pastorekova S, Parkkila S, Parkkila AK, Opavsky R, Zelnik V, Saarnio J, et al. Carbonic anhydrase IX, MN/CA IX: analysis of stomach complementary DNA sequence and expression in human and rat alimentary tracts. Gastroenterology 1997;112:398–408.
17. Liao SY, Rodgers WH, Kauderer J, Bonfiglio TA, Walker JL, Darcy KM, et al. Carbonic anhydrase IX and human papillomavirus as diagnostic biomarkers of cervical dysplasia/neoplasia in women with a cytologic diagnosis of atypical glandular cells: a Gynecologic Oncology Group study in United States. Int J Cancer 2009;125: 2434–40.
18. Gut MO, Parkkila S, Vernerova Z, Rohde E, Zavada J, Hocker M, et al. Gastric hyperplasia in mice with targeted disruption of the carbonic anhydrase gene Car9. Gastroenterology 2002;123:1889–903.
19. Chia SK, Wykoff CC, Watson PH, Han C, Leek RD, Pastorek J, et al. Prognostic significance of a novel hypoxia-regulated marker, carbonic anhydrase IX, in invasive breast carcinoma. J Clin Oncol 2001;19:3660–8.
20. Giatromanolaki A, Koukourakis MI, Sivridis E, Pastorek J, Wykoff CC, Gatter KC, et al. Expression of hypoxia-inducible carbonic anhydrase-9 relates to angiogenic pathways and independently to poor outcome in non-small cell lung cancer. Cancer Res 2001; 61:7992–8.
21. Watson PH, Chia SK, Wykoff CC, Han C, Leek RD, Sly WS, et al. Carbonic anhydrase XII is a marker of good prognosis in invasive breast carcinoma. Br J Cancer 2003;88:1065–70.
22. Casanovas O, Hicklin DJ, Bergers G, Hanahan D. Drug resistance by evasion of antiangiogenic targeting of VEGF signaling in late-stage pancreatic islet tumors. Cancer Cell 2005;8:299–309.
23. Jain RK, Duda DG, Clark JW, Loeffler JS. Lessons from phase III clinical trials on anti-VEGF therapy for cancer. Nat Clin Pract Oncol 2006;3:24–40.
24. Li JL, Sainson RC, Shi W, Leek R, Harrington LS, Preusser M, et al. Delta-like 4 Notch ligand regulates tumor angiogenesis, improves tumor vascular function, and promotes tumor growth *in vivo*. Cancer Res 2007;67:11244–53.
25. Bergers G, Hanahan D. Modes of resistance to anti-angiogenic therapy. Nat Rev Cancer 2008;8:592–603.
26. Ebos JM, Lee CR, Kerbel RS. Tumor and host-mediated pathways of resistance and disease progression in response to antiangiogenic therapy. Clin Cancer Res 2009;15:5020–5.
27. Hong YS, Cho HJ, Kim SY, Jung KH, Park JW, Choi HS, et al. Carbonic anhydrase 9 is a predictive marker of survival benefit from lower dose of bevacizumab in patients with previously treated metastatic colorectal cancer. BMC Cancer 2009;9:246.
28. Sathornsumetee S, Cao Y, Marcello JE, Herndon JE II, McLendon RE, Desjardins A, et al. Tumor angiogenic and hypoxic profiles predict radiographic response and survival in malignant astrocytoma patients treated with bevacizumab and irinotecan. J Clin Oncol 2008;26:271–8.
29. Reardon DA, Desjardins A, Vredenburgh JJ, Gururangan S, Sampson JH, Sathornsumetee S, et al. Metronomic chemotherapy with daily, oral etoposide plus bevacizumab for recurrent malignant glioma: a phase II study. Br J Cancer 2009;101:1986–94.
30. Chiche J, Ilc K, Laferriere J, Trottier E, Dayan F, Mazure NM, et al. Hypoxia-inducible carbonic anhydrase IX and XII promote tumor cell growth by counteracting acidosis through the regulation of the intracellular pH. Cancer Res 2009;69:358–68.
31. Lou Y, McDonald PC, Oloumi A, Chia SK, Ostlund C, Ahmadi A, et al. Targeting tumor hypoxia: suppression of breast tumor growth and metastasis by novel carbonic anhydrase IX inhibitors. Cancer Res 2011;71:3364–76.
32. Ivascu A, Kubbies M. Rapid generation of single-tumor spheroids for high-throughput cell function and toxicity analysis. J Biomol Screen 2006;11:922–32.
33. Harrington LS, Sainson RC, Williams CK, Taylor JM, Shi W, Li JL, et al. Regulation of multiple angiogenic pathways by Dll4 and Notch in human umbilical vein endothelial cells. Microvasc Res 2008;75: 144–54.
34. Wykoff CC, Beasley N, Watson PH, Campo L, Chia SK, English R, et al. Expression of the hypoxia-inducible and tumor-associated carbonic anhydrases in ductal carcinoma *in situ* of the breast. Am J Pathol 2001;158:1011–9.
35. Ruifrok AC, Johnston DA. Quantification of histochemical staining by color deconvolution. Anal Quant Cytol Histol 2001;23:291–9.
36. Khalifah RG. The carbon dioxide hydration activity of carbonic anhydrase. I. Stop-flow kinetic studies on the native human isoenzymes B and C. J Biol Chem 1971;246:2561–73.
37. Swietach P, Vaughan-Jones RD, Harris AL. Regulation of tumor pH and the role of carbonic anhydrase 9. Cancer Metastasis Rev 2007;26:299–310.
38. Swietach P, Hulikova A, Vaughan-Jones RD, Harris AL. New insights into the physiological role of carbonic anhydrase IX in tumour pH regulation. Oncogene 2010;29;6509–21.
39. Svastova E, Zilka N, Zat'ovicova M, Gibadulinova A, Ciampor F, Pastorek J, et al. Carbonic anhydrase IX reduces E-cadherin-mediated adhesion of MDCK cells via interaction with beta-catenin. Exp Cell Res 2003;290:332–45.
40. Dorai T, Sawczuk IS, Pastorek J, Wiernik PH, Dutcher JP. The role of carbonic anhydrase IX overexpression in kidney cancer. Eur J Cancer 2005;41:2935–47.
41. Griffiths JR. Are cancer cells acidic? Br J Cancer 1991;64:425–7.
42. Gatenby RA, Gawlinski ET, Gmitro AF, Kaylor B, Gillies RJ. Acid-mediated tumor invasion: a multidisciplinary study. Cancer Res 2006;66:5216–23.
43. Alterio V, Hilvo M, Di Fiore A, Supuran CT, Pan P, Parkkila S, et al. Crystal structure of the catalytic domain of the tumor-associated human carbonic anhydrase IX. Proc Natl Acad Sci U S A 2009;106:16233–8.
44. Leek RD, Landers RJ, Harris AL, Lewis CE. Necrosis correlates with high vascular density and focal macrophage infiltration in invasive carcinoma of the breast. Br J Cancer 1999;79:991–5.
45. Condeelis J, Pollard JW. Macrophages: obligate partners for tumor cell migration, invasion, and metastasis. Cell 2006;124:263–6.
46. Pollheimer MJ, Kornprat P, Lindtner RA, Harbaum L, Schlemmer A, Rehak P, et al. Tumor necrosis is a new promising prognostic factor in colorectal cancer. Hum Pathol 2010;41:1749–57.

Published OnlineFirst April 12, 2012; DOI:10.1158/1078-0432.CCR-11-1877

47. Scholzen T, Gerdes J. The Ki-67 protein: from the known and the unknown. J Cell Physiol 2000;182:311–22.
48. Zavada J, Zavadova Z, Zat'ovicova M, Hyrsl L, Kawaciuk I. Soluble form of carbonic anhydrase IX (CA IX) in the serum and urine of renal carcinoma patients. Br J Cancer 2003;89:1067–71.
49. Davis ID, Wiseman GA, Lee FT, Gansen DN, Hopkins W, Papenfuss AT, et al. A phase I multiple dose, dose escalation study of cG250 monoclonal antibody in patients with advanced renal cell carcinoma. Cancer Immun 2007;7:13.
50. Guzel O, Maresca A, Scozzafava A, Salman A, Balaban AT, Supuran CT. Carbonic anhydrase inhibitors. Synthesis of 2,4,6-trimethylpyridinium derivatives of 2-(hydrazinocarbonyl)-3-aryl-1H-indole-5-sulfonamides acting as potent inhibitors of the tumor-associated isoform IX and XII. Bioorg Med Chem Lett 2009;19:2931–4.